



Contents lists available at ScienceDirect

## Journal of Sound and Vibration

journal homepage: [www.elsevier.com/locate/jsvi](http://www.elsevier.com/locate/jsvi)

## Critical insights for advanced bridge scour detection using the natural frequency



Ting Bao<sup>a</sup>, R. Andrew Swartz<sup>b</sup>, Stanley Vitton<sup>c</sup>, Ye Sun<sup>d</sup>, Chao Zhang<sup>e</sup>, Zhen Liu<sup>f,\*</sup>

<sup>a</sup> Department of Civil and Environmental Engineering, Michigan Technological University, 1400 Townsend Drive, Dow 854, Houghton, MI 49931, United States

<sup>b</sup> Department of Civil and Environmental Engineering, Michigan Technological University, 1400 Townsend Drive, Dillman 201D, Houghton, MI 49931, United States

<sup>c</sup> Department of Civil and Environmental Engineering, Michigan Technological University, 1400 Townsend Drive, Dillman 201G, Houghton, MI 49931, United States

<sup>d</sup> Department of Mechanical Engineering and Engineering Mechanics, Michigan Technological University, 1400 Townsend Drive, MEEM 926, Houghton, MI 49931, United States

<sup>e</sup> Department of Civil and Environmental Engineering, Michigan Technological University, 1400 Townsend Drive, Dow 823, Houghton, MI 49931, United States

<sup>f</sup> Department of Civil and Environmental Engineering, Michigan Technological University, 1400 Townsend Drive, Dillman 201F, Houghton, MI 49931, United States

### ARTICLE INFO

#### Article history:

Received 22 June 2015

Received in revised form

16 June 2016

Accepted 28 June 2016

Handling Editor: I. Trendafilova

Available online 4 October 2016

#### Keywords:

Predominant natural frequency Scour detection

Physical meaning

Sensor installation

Scour hole shape

### ABSTRACT

Scour around bridge foundations is regarded as one of the predominant causes of bridge failures. The concept of vibration-based real-time bridge scour detection has been explored in recent years by investigating the change in the natural frequency spectrum of a bridge or a bridge component with respect to the scour depth. Despite the progress, significant issues still remain unsolved in the application of this concept. This paper investigates three unsolved issues in the current framework of scour detection using the natural frequency spectrum: the physical meaning of the measured predominant natural frequency, the location of sensor installation, and the influence of the shape of scour holes, which are easily neglected but critical to the further implementations of the natural frequency spectrum-based bridge scour detection. Firstly, in-depth discussions of these three major issues were made separately by numerically modeling the scour progression of a typical and documented laboratory test. Laboratory tests were then performed to validate the conclusions made in the discussions. It was found that for an eigenproblem of the system with soil-structure interaction, the physical meaning of the natural frequency obtained from modal analysis can be understood by comparing the modal natural frequency with the natural frequency calculated from the dynamic response of the test component in that system. The results also verified that the obtained predominant natural frequency of the pier body greatly varies with the location of the pier body where a sensor is mounted for signal pickup. The shape of the scour hole affects the predominant natural frequency of the pier, causing difficulties in practical measurements. To address such a

\* Corresponding author.

E-mail addresses: [tbao@mtu.edu](mailto:tbao@mtu.edu) (T. Bao), [raswartz@mtu.edu](mailto:raswartz@mtu.edu) (R. Andrew Swartz), [vitton@mtu.edu](mailto:vitton@mtu.edu) (S. Vitton), [yes@mtu.edu](mailto:yes@mtu.edu) (Y. Sun), [c Zhang26@mtu.edu](mailto:c Zhang26@mtu.edu) (C. Zhang), [zhenl@mtu.edu](mailto:zhenl@mtu.edu) (Z. Liu).

problem, a new criterion was proposed to identify the depth of unsymmetrical scour holes for the first time, which is of practical significance to advance the natural frequency spectrum-based scour detection framework.

© 2016 Elsevier Ltd. All rights reserved.

## 1. Introduction

Scour around bridge foundations is regarded as one of the predominant factors in inducing bridge failures [1], which seriously threatens the bridge safety as scour weakens bridge foundations by removing soils around them. To avoid this threat, numerous investigations have been made to predict scour severity. The most straightforward way is to estimate scour situations using empirical equations. Factors such as construction methods, scour models, and site conditions can be included in the empirical equations [2,3]. Stochastic approaches were also proposed to evaluate scour severity considering small errors and correlation coefficients [4,5]. As a result, the predicted results using these stochastic methods are more satisfactory than those using the empirical equations [4].

Numerical simulations, laboratory modeling, and in situ monitoring have also been used to evaluate bridge scour. The complicated scour process involving soil–fluid–structure interaction has been simulated using numerical models [6,7]; while the real situations affected by the water flow and soil interaction have been modeled in laboratory tests [8,9]. Results from both of these numerical simulations and laboratory tests can be utilized to better understand the effect of different factors on the scour development. Another direct and effective way is to use sensors and instruments in situ to detect scour progression. Sensors and instruments such as Fiber-Bragg Grating sensors and buried driven rods were applied for long term scour evolution monitoring [10,11].

A novel method based upon vibration to detect scour severity has been gaining momentum in recent years. The main advantage of this method is that it only requires a simple sensor such as an accelerometer to be installed at a bridge pier rather than expensive underwater instrument installation [12]. Previous underwater instruments such as float-out devices and Time Domain Reflectometry (TDR) sensors need to be positioned in the soil near a bridge pier before monitoring [13,14]. Also, TDRs are susceptible to environmental conditions such as temperature and radiation [14]. Instruments such as Ground Penetrating Radars cannot be used for continuous scour monitoring due to the limitations [15]. However, vibration-based bridge scour detection can address such limitations by investigating the variation of the natural frequency spectrum with respect to scour severity, which possibly provides a more effective way to detect bridge scour progression.

Many investigations have explored this novel scour detection concept based on the hypothesis that scour has an effect on the natural frequency spectrum of a bridge component such as a pier. One typical approach is to install a sensor at a bridge pier, either in the laboratory or in situ, to record its dynamic response generated by forced vibration. The change in the Predominant Natural Frequency (PNF), which is the main target for scour evaluation, is obtained by transferring the dynamic data from the time domain into the frequency domain using the Fast Fourier Transform (FFT) [12,16]. The other approach is to obtain the PNF by numerically modeling simplified lab-scale or full-scale bridges. The change in the PNF can then be obtained directly from simulations using modal analysis [17,18]. Despite the progress, unsolved issues still remain in both theoretical and practical aspects of vibration-based bridge scour detection.

To advance the topic, this paper discusses three easily neglected but critical issues in the current framework of implementing bridge scour detection using the natural frequency spectrum. 1. For an eigenproblem of a system with soil–structure interaction, the natural frequency obtained from the modal analysis in the designated direction (e.g., flow direction) was considered as the PNF of the bridge or the bridge pier of that system in that direction for scour detection [18]. It is unclear whether this PNF belongs to a bridge component such as a pier, to soils, or to the whole computational domain. 2. The dynamic response is obtained by sensors at some points at bridge components such as a pier or a deck for practical scour measurements [12,19]. However, little attention has been paid to the question, “Where is the best location of sensor installation?” 3. Previous simulations considered the change in the PNF with the development of symmetrical scour holes [12,20]. However, there has been no discussion on the effect of the unsymmetrical shape of scour holes on the PNF. In this paper, these three unsolved issues were discussed separately with numerical studies, which were validated against a documented laboratory test before the discussions. Then, laboratory tests were performed to validate the conclusions obtained in the discussions based on the numerical simulations.

## 2. A numerical model and its validation

The natural frequency spectrum of a bridge pier is affected by its boundary conditions. As scour changes the boundary conditions by removing the soil around the pier, bridge scour can be detected by observing the change in the natural frequency spectrum. In this section, a theoretical model is presented to simulate an existing scour laboratory test with assistance of a finite element program, ABAQUS. The accuracy of the numerical model was validated by comparing the simulation results with documented experimental results.

## 2.1. Theoretical formulation

The natural frequency of a multiple-degree-of-freedom system can be calculated by employing the dynamic equation of motion as shown below [21]:

$$[\mathbf{M}]\ddot{\mathbf{x}} + [\mathbf{C}]\dot{\mathbf{x}} + [\mathbf{K}]\mathbf{x} = \mathbf{F} \quad (1)$$

where  $[\mathbf{M}]$ ,  $[\mathbf{C}]$  and  $[\mathbf{K}]$  are the mass, damping, and stiffness matrices, respectively;  $\mathbf{x}$  is the displacement vector;  $\ddot{\mathbf{x}}$  and  $\dot{\mathbf{x}}$  are the acceleration and velocity vectors respectively;  $\mathbf{F}$  is the external force vector. The matrices are  $N \times N$  square matrices where  $N$  is the number of degrees of freedom of the system.

To solve Eq. (1), one strategy is to convert Eq. (1) to the free dynamic equation of motion by neglecting the damping matrix  $[\mathbf{C}]$  and the external force  $\mathbf{F}$ . Assuming  $\mathbf{x} = \{\phi\}e^{i\omega t}$  [21], one obtains an eigenproblem:

$$[-\omega^2[\mathbf{M}] + [\mathbf{K}]]\{\phi\} = \mathbf{0} \quad (2)$$

where  $\omega_r$  ( $0 \leq \omega_1 < \omega_2 < \dots < \omega_N$ ) is the  $r_{th}$  natural frequency of the system, which corresponds to a mode shape of the system in each direction. If the  $r_{th}$  mode shape appears in the designated direction, the corresponding natural frequency is used to represent the natural frequency in that direction. To accomplish this, the Lanczos method can be used to solve the symmetric eigenproblem [22]. This can be done by converting the original eigenproblem to the standard eigenproblem of a triple diagonal matrix based on the Lanczos algorithm:

$$[\mathbf{Z}][\mathbf{L}] - [\mathbf{L}]\lambda = \mathbf{0} \quad (3)$$

where  $[\mathbf{Z}]$  and  $\lambda$  are the arrays of eigenvectors and eigenvalues, respectively;  $[\mathbf{L}]$  is a triple diagonal matrix. By solving Eq. (3), one can obtain  $\lambda$ , which are not eigenvalues of the original eigenproblem. However, one can convert  $\lambda$  to the natural frequency  $\omega$  of the original eigenproblem using the following equation:

$$\omega_r^2 = 1/\lambda_r \quad (4)$$

where  $\lambda_r$  is the  $r_{th}$  eigenvalue in the eigenvalue array,  $\lambda$ . The other way to obtain the natural frequency of the system with damping effects is to analyze its dynamic responses to a given impulse force by applying an impulse force  $\mathbf{F}_{ext}$  to Eq. (1). According to Craig and Kurdila [21], the damping matrix can be defined as Rayleigh damping:

$$[\mathbf{C}] = \alpha[\mathbf{M}] + \beta[\mathbf{K}] \quad (5)$$

where  $\alpha$  and  $\beta$  are the arbitrary proportional coefficients, which are related to the damping ratio of the system. The damping ratio can be evaluated using a relatively straightforward exponential curve fitting method [23].

According to Chopra [24], it is advantageous to transform Eq. (1) into modal coordinates in the typical way of the displacement vector transformation [25]. By using the orthogonal condition of the mode shape matrices, a set of the  $N$  coupled equations in nodal displacements is transformed to a set of the  $N$  uncoupled equations in modal coordinates. The direct integration method then can be used to solve these  $N$  uncoupled equations to obtain the dynamic response of each mode shape [21]. One obtains the dynamic responses of the system by superimposing the dynamic response of each mode shape as below:

$$\mathbf{u}(t) = \sum_{i=1}^N \phi_i x_i(t) \quad (6)$$

where  $\phi_i$  is the displacement vector and  $x_i$  is the displacement. Accordingly, the velocity variation and acceleration variation with respect to time are given via the first and second derivative of Eq. (6), respectively. Therefore, the natural frequency can be obtained by transforming the dynamic data from the time domain into the frequency domain using the FFT.

## 2.2. Implementations

### 2.2.1. Model implementations

The scour progression was studied by numerically simulating a typical scour laboratory test. The numerical model was solved with assistance of the commercial finite-element program, ABAQUS. This program provides an eigenvalue analysis model to identify the Predominant Mode Shape (PMS) which corresponds to the PNF of the model. Based on that, the variation of the PNF with respect to the scour development can be obtained to assess scour severity. The simulation results based on the numerical model were then validated against this lab-scale test.

Briaud et al. [18] conducted a typical scour experiment to measure the change in the natural frequency spectrum of a pier with a shallow foundation. As shown in Fig. 1, this experiment simulated a system with one pier and two decks. A concrete column, 0.45 m and 4 m in diameter and length, respectively, was used as a down-scaled pier and two prefabricated concrete decks, 0.53 m wide, 2.03 m long, and 0.1 m thick, were installed end-to-end on the top of the column to simulate bridge decks. The concrete column was embedded into a sand block (9 m long, 3.6 m wide and 1.5 m deep) in a 2D flume to model a shallow foundation. Multiple sensors were set up to record experimental data with the development of scour,

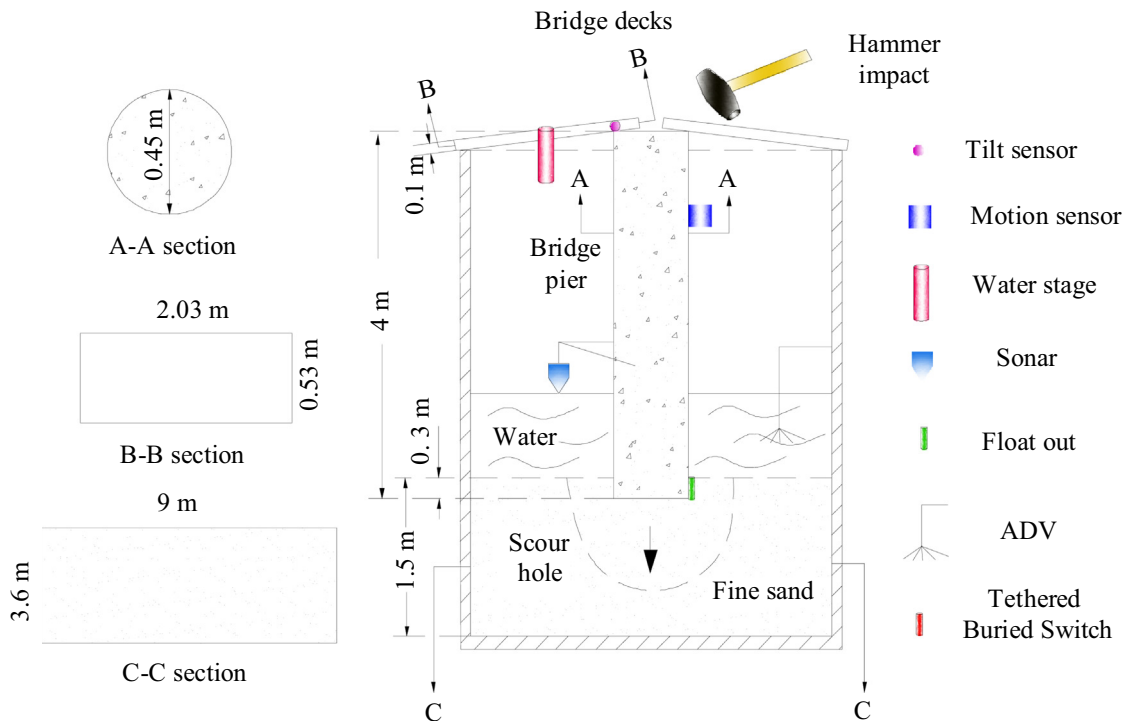


Fig. 1. Schematic of scour detection in the shallow foundation [reproduced from Briaud et al. [18]].

among which a motion sensor was installed at the position about 0.8 m away from the top surface of the pier to record its dynamic responses.

The test [18] was performed in several steps. First, a hammer was used to generate vibration when the flume was not filled up with water. Then, the flume was filled up with water and vibration was generated by a flow, in which different flow velocities were tested. A bridge scour hole was developed as the flow velocity increased. When the scour hole reached the bottom of the pier, the pier started to settle and rock. Finally, a conical shape scour hole was formed. The variation in the PNF of the pier in the flow direction was obtained by means of the FFT of the dynamic responses of the pier measured using the motion sensor.

Numerical simulations were conducted based on this scour detection experiment using the identical geometry, material properties, and boundary conditions to investigate the change in the PNF with the scour development. The decks and concrete pier were assumed to be elastic and homogeneous, which were modeled by a standard 20-node quadratic brick element with quadratic geometric order. To represent the soil-pier behavior, the dimensions of the soil mesh was twice of the pier dimensions in the horizontal plane [17]. A perfectly plastic Mohr-Coulomb model was used as the constitutive relationship for the soil, which was also modeled by a standard 20-node quadratic brick element with quadratic geometric order. The soil cohesion and the angle of soil internal friction for this plastic model were 0 and  $37^\circ$ , respectively. The soil elastic modulus and bulk density were 12 MPa and  $1928 \text{ kg/m}^3$ , respectively. The water was not included in this model as the effect of water on the PNF is possibly negligible according to the existing studies [12,17]. Prendergast et al. [12] conducted a laboratory investigation to estimate the effect of water on measured PNFs of three cantilever structures with varying cross-sectional stiffness. It was found that the percentage difference in the measured PNFs of the stiff cantilever structure with and without water was 0.3 percent. Also, the simulation results obtained by Ju [17] for a full-scale bridge involving the fluid-structure interaction showed that water affected the PNF. However, the PNFs calculated with and without the fluid-structure interaction were not obvious. Therefore, the effect of water is assumed to be negligible when measuring the PNF of a pier in this study. Fig. 2 shows the mesh of the 3D Finite Element Model (FEM) without scour and that with a developed scour hole.

The contact between components is a significant factor as the PNF of a pier is significantly affected by the constraint of the soils around the pier. This model involves three different pairs of contacts, i.e., deck-support contact, deck-pier contact, and pier-soil contact. To obtain a representative soil-pier interaction, a penalty method was used in the tangential direction and a hard contact method was used in the normal direction. The reason is that the pier elements connect with the surrounding soil elements. The hard contact is a typical approach for facilitating convergence when modeling the contact pressure between two surfaces in the normal direction; while the penalty method is a stable approach to simulate the contacts between different elements of dissimilar materials [18]. The same approach was applied to the deck-pier contact. A frictionless method in the tangential direction was used to model the deck-support contact and the hard contact was

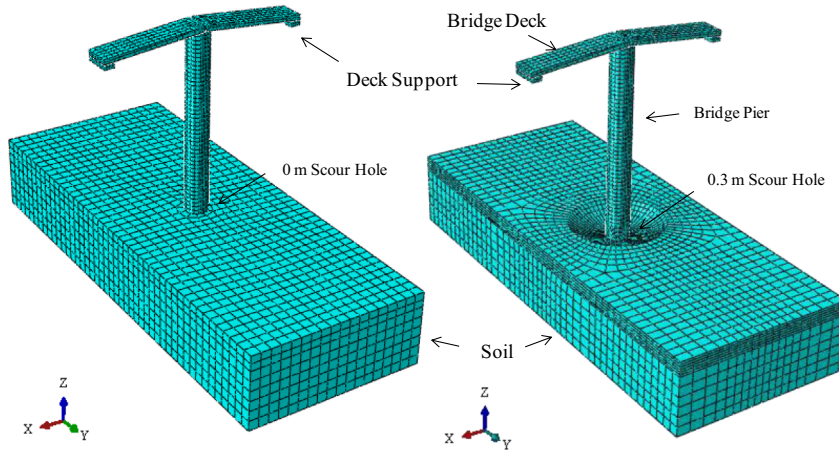


Fig. 2. 3D FEM without scour and with a developed scour hole.

applied in the normal direction.

The boundary condition is another vital factor to the behavior of the model. All boundary conditions were defined to ensure the similarity to the experiment. A roller boundary condition was used on the four side faces and the base of the soil block to simulate the condition in the experiment where the soil was surrounded by concrete walls. All the boundaries of the deck support were fixed. No constraint was applied to the bridge deck and the bridge pier, except the aforementioned contacts. The Lanczos solver was used to compute the eigenproblem of this coupled model and to extract its PNF. Scour situations were simulated by symmetrically removing the soil around the pier to induce a reserve-cone-shape scour hole as shown in Fig. 2.

2.2.2. Results and validations

Two scenarios were simulated in terms of the corresponding periods in the experiment. As shown in Fig. 3, Period AB starting from Point A to Point B corresponds to the process from the scour depth of 0 m to 0.3 m. The scour depths were modeled based on the assumption that there was no settlement but a contact (bottom of the pier) between the pier and the soil. The increment was 0.03 m in each step. All other constraints remained unchanged. Period BC starting from Point B to Point C corresponds to the situation beyond the scour depth of 0.3 m, which was the final scour measurement in the experiment. The pier started to settle and the deck started to move downward after Point B. The final scour depth was about 0.42 m which was greater than the maximum scour depth of 0.3 m in Period AB. Therefore, all constraints in Period AB changed in Period BC; thus, it was difficult to model the experimental process after Point B. To avoid confusion, this study just analyzed the final situation by removing the contact between the bottom of the pier and the soil.

The documented experimental results in Fig. 3 were used to validate the numerical solutions. For completeness, the numerical results in this study were also compared with the previous simulation results of Briaud et al. [18]. Fig. 4 plots the comparison between the first PNF obtained from the current model and the experimental results, as well as the previous simulation results from Briaud et al. [18] for both Periods AB and BC. The current PNF values are 9.38 Hz and 8.93 Hz at Point

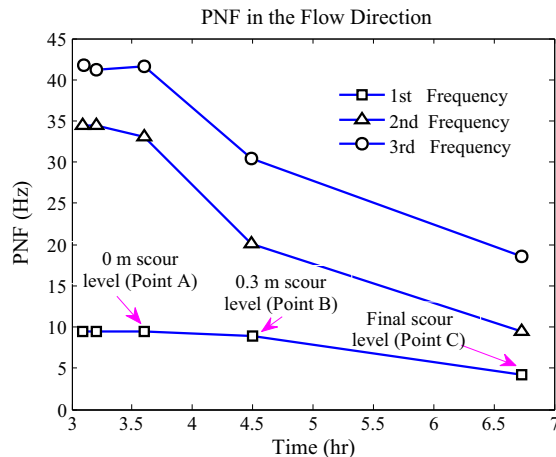
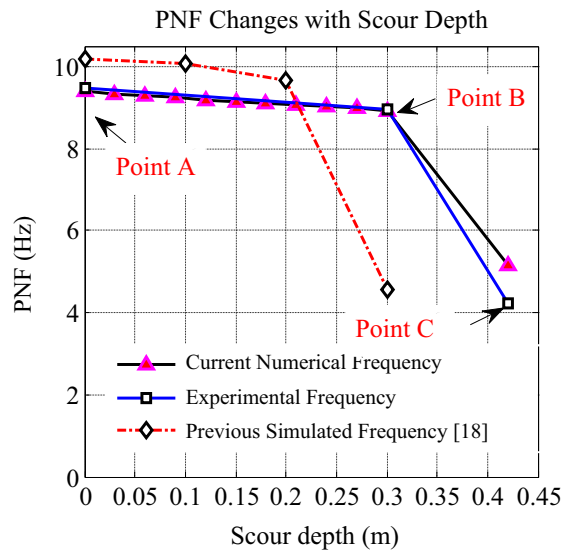


Fig. 3. Variation of the PNF with time in the experiment [reproduced from Briaud et al. [18]].



**Fig. 4.** Comparison between the current numerical PNF and experimental PNF and numerical PNF of Briaud et al. [18]. (For interpretation of the references to color in this figure, the reader is referred to the web version of this article.)

A and B, respectively, which are very close to the experimental values of 9.49 Hz and 8.97 Hz, while the simulation results of Briaud et al. [18] are not in agreement with the experimental values. For the scour depth of 0.3 m (Point B), it was assumed that the soil-pier contact at the bottom of the pier still worked in the current simulations. This assumption matches with the experiment because the pier started to settle and rock after Point B which is the critical point between Periods AB and BC.

The current numerical PNF decreases dramatically for Period BC as shown in Fig. 4. This trend agrees with the observed experimental results. However, only one numerical value at Point C was plotted due to the fact that the pier and the deck started settling down after Point B. The pier constraints changed with its settlement during Period BC, but Period BC was neglected in the previous simulations (the red dashed line), which assumed Period AB to be the whole scour development. As shown in Fig. 4, the black line matches the blue line better when compared to the red dashed line. Thus, the current simulations yield better results than the previous simulations. This is possibly because the current model builds precise contacts between the components. Also, the current model reflects the experimental process more in detail rather than neglects the critical Point B.

### 3. Critical issues and discussions

#### 3.1. Issue 1: physical meaning of the PNF obtained from modal analysis

The numerical model introduced and validated in the previous section was employed to investigate three critical issues in the theoretical and practical aspects of PNF-based bridge scour detection. The first issue is the physical meaning of the PNF obtained from the modal analysis, which will be discussed in this section. By applying the modal analysis, the PNF is obtained by identifying the PMS of the system in a designated direction. However, it is always of scientific and practical significance to ask, "What does the PNF belong to, a component, e.g., a pier, soils, or the whole computational domain?" In field tests, the PNF of a bridge component can be used to detect bridge scour. However, in numerical simulations, the natural frequency corresponding to the PMS in a designated direction (e.g., flow direction) is usually used as the PNF of a bridge pier in that direction, but it is difficult to identify the PMS of a pier for an eigenproblem with the soil-pier interaction because this mode shape may be due to soil modal displacements. The pier will also move with the soil modal displacements in the same direction due to the soil-pier interaction, but the soil-induced mode shape cannot be represented as the PMS of the pier to obtain the PNF for scour detection [17]. Irrational evaluations may result in false measurements by choosing an unreasonable mode shape as the PMS of a pier.

To investigate this issue, a modal analysis was first performed to preliminarily assess the change in the PNF of the pier due to progressive scour. Table 1 shows the natural frequency of the first three mode shapes of the system at scour depths from 0 m to 0.09 m. The PNF corresponding to the second mode shape appeared in the traffic direction where the modal displacements of the second mode shape are parallel to the bridge deck, which will not be discussed in this study. This section investigates the PNF corresponding to the mode shape in the flow direction where its modal displacements are perpendicular to the bridge deck. This is because the modal displacements of the pier in the flow direction are attributable to both the first and third mode shapes. The concept of PNF-based scour detection is to measure the change in the PNF of the pier. Based on previous studies, the PNF of a concrete pier changes with scour progression in a small range of the value such

**Table 1**  
Identified PNFs of mode shapes.

Scour depth (m)	PNF of mode shapes (Hz)			Difference in PNF between 1st and 3rd (Hz)
	1st	2nd	3rd	
0	8.84	9.05	9.38	0.54
0.03	8.81	9.03	9.33	0.52
0.06	8.78	9.00	9.28	0.50
0.09	8.74	8.98	9.24	0.50

as 0.5 Hz within a scour depth of 0.3 m [18]. As shown in Table 1, the difference between the PNFs corresponding to the first mode shape and the third mode shape is around 0.52 Hz for these scour depths. This phenomenon leads to a difficulty in identifying that the PNF corresponding to which mode shape belongs to the pier rather than the soils or the whole computational domain. This difficulty is also proposed in the study of Ju [17]. To solve such a difficulty, the PNF calculated from the dynamic responses was used to identify the physical meaning of the PNF obtained from the first and third mode shapes.

The method of the dynamic responses of the pier was implemented via a process in which transient signals such as the variation of acceleration with time were transformed from the time domain into the frequency domain using the FFT. In the field test, the PNF of a pier calculated from the dynamic responses is used to detect scour [19,26], but the modal analysis cannot be practically used in the field directly. Based on the classic theory described in the theoretical section, the PNF extracted from the modal analysis should be equal to that calculated from the dynamic responses of the pier. Therefore, the problem proposed in this section can be understood by comparing the PNF extracted from the modal analysis with that calculated from the dynamic responses. To obtain the dynamic responses of the pier, a 500 N concentrated force was used to generate 0.01 s duration of vibration. This transient duration can eliminate the effect of forced vibration considerably [27]. The surface position on the pier where a sensor was installed in the experiment, as shown in Fig. 1, was selected as the location to obtain the dynamic responses of this pier.

Fig. 5a shows the PNFs obtained from the dynamic responses of the pier (dynamic PNF) at different scour depths using the FFT. There is an explicit reduction in the dynamic PNF changing from 9.40 Hz to 8.96 Hz. Fig. 5b plots the correlation between the dynamic PNFs obtained in Fig. 5a and the PNFs corresponding to the first and third mode shapes. For dynamic PNF validations, the experimental PNFs of Point A and Point B in Fig. 4 were also plotted in Fig. 5b. As can be seen, the dynamic PNF is in agreement with the natural frequency corresponding to the third mode shape rather than that of the first mode shape. The dynamic PNFs also agree well with the experimental PNFs. The results confirmed that the third mode shape belongs to the pier while the first mode shape belongs to the soils. The reason is that the third mode shape of the coupled model primarily contributes to the modal deformation of the pier. Thus, the corresponding natural frequency of this mode can be confirmed as the PNF of the pier to evaluate scour severity. This conclusion further validates the accuracy of the model developed in this study.

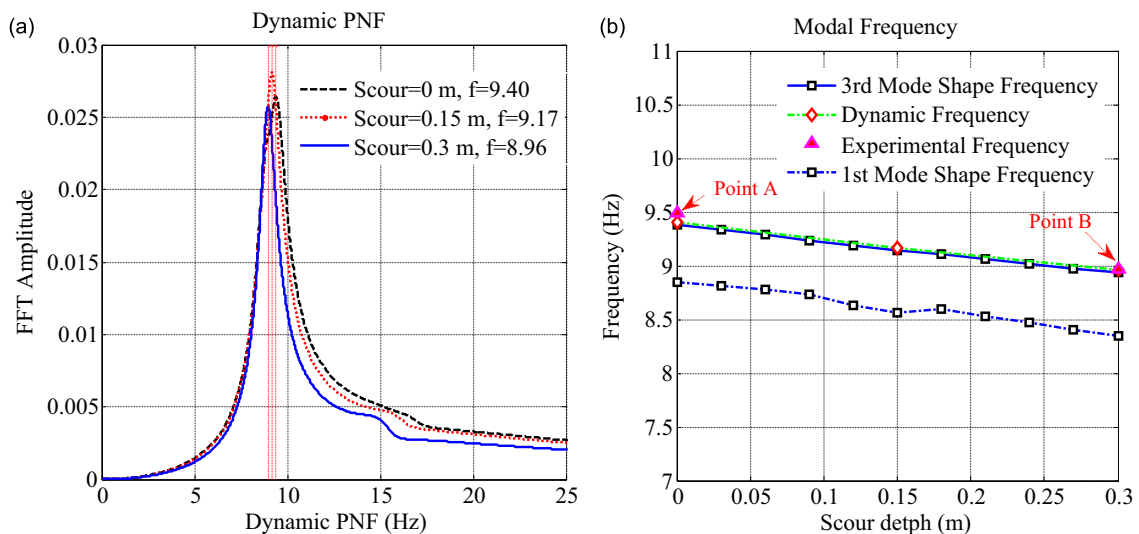


**Fig. 5.** Comparison between the mode shape and dynamic natural frequency: (a) the dynamic PNF at different scour depths; (b) correlation between the modal PNF and dynamic PNF.

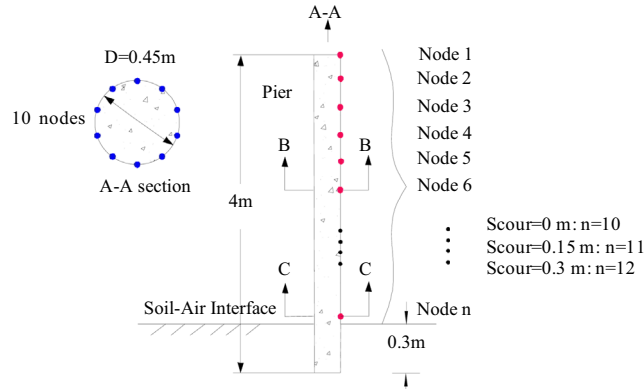


Fig. 6. Schematic of nodes chosen for analysis.

3.2. Issue 2: location of sensor installation

The second issue is the location of sensor installation, which is of practical importance as an inappropriate location may lead to false measurements, and an optimal location also ensures better accessibility and signal pickup. In either field or experimental tests, the dynamic response is usually obtained with sensors at some surface points of bridge components such as a pier and a deck [12,19]. Measuring the dynamic response, e.g., the variation of acceleration with time, from these points using sensors is equivalent to abstracting numerical results from the corresponding points. However, there has been rare research on where the valid or the best location (s) of sensor installation is. To this end, the dynamic PNFs obtained at different points of the pier body were compared. Different nodes in two directions, i.e., horizontal and vertical direction, were studied at scour depths of 0 m, 0.15 m, and 0.3 m.

Fig. 6 illustrates the nodes chosen for the comparison study. For the vertical direction, nodes were selected along the vertical axis on one side of the pier. For the horizontal direction, three cross sections were defined, i.e., A-A (top), B-B (middle), and C-C (bottom), in which 10 different nodes were studied in each section. All nodes from the two directions were selected with equal increments at the same scour depth. Therefore, the selected nodes in the horizontal and vertical directions can cover all representative locations of sensor installation for this cylinder pier. Fig. 7 plots the PNFs in three cross sections of the pier. The PNFs remain unchanged if the selected nodes are in the same cross section. However, the PNFs are not the same in different cross sections. The PNFs in the cross section of C-C are obviously greater than those of A-A and B-B; while the PNFs in the cross section of B-B are slightly greater than those of A-A. Because of this difference, it is necessary to analyze the difference in the PNFs of the selected nodes along the pier in the vertical direction. Fig. 8 presents the variation of the dynamic PNFs at different nodes along the vertical direction. The PNFs at the nodes along the vertical direction do not remain the same. A sudden change appears at a location close to the bottom of the pier in all the three cases. The reason is that points at the same horizontal plane have identical properties due to the uniform properties within the pier. The PNF depends on the stiffness and mass, which results in an identical PNF in the same horizontal cross section. However, there is a difference in the stiffness of points selected from different positions in the pier body. The stiffness tends

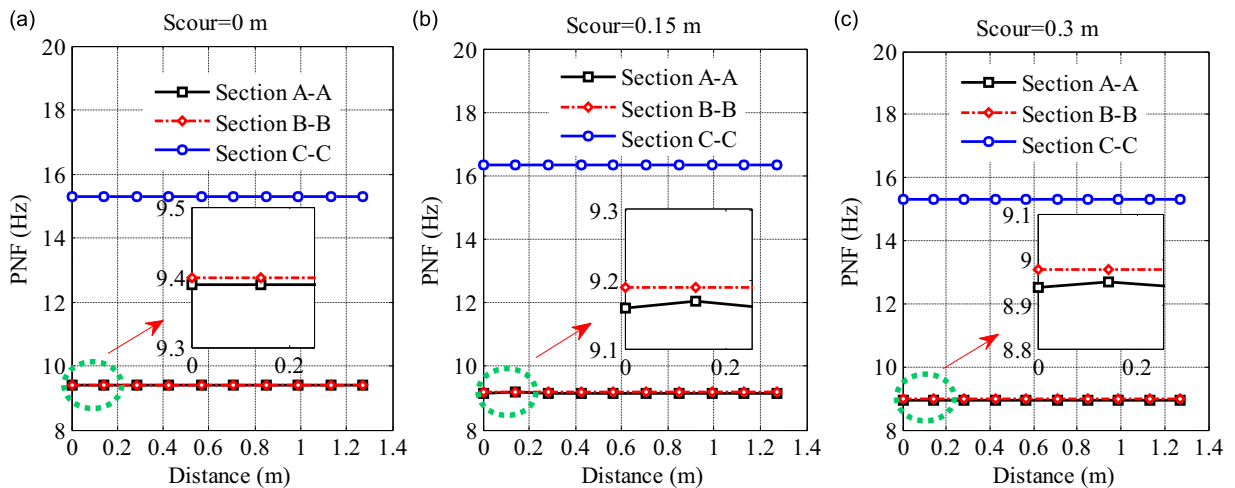


Fig. 7. Variation of the PNF along the horizontal direction.

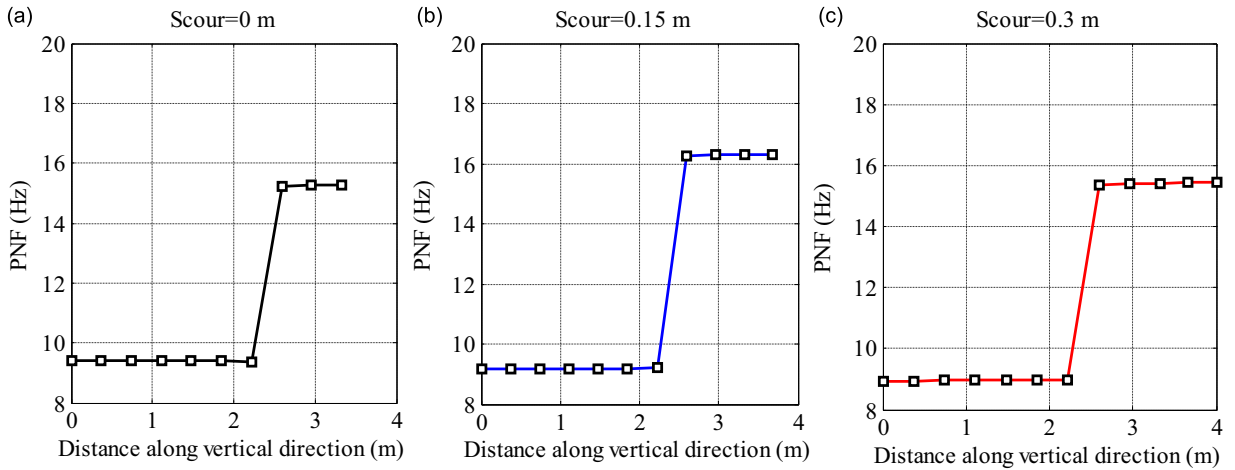


Fig. 8. Variation of the PNF along the vertical direction.

to be greater when the selected points are at locations close to the bottom, which leads to the low value of the PNF obtained at the top of the pier and the high value of the PNF obtained at the bottom of the pier. This is because the effect of constraints by soils at these locations is larger than those on the top. The obtained PNFs at the top or bottom of the pier therefore are much different.

### 3.3. Issue 3: Influence of the Shape of Scour Holes

The third issue is the influence of the shape of scour holes on the PNF of the pier, which has not been discussed before either. Previous numerical and experimental studies have simulated scour scenarios by removing a surface soil layer or soils around bridge foundations [12,18,20]. The shape of these scour holes is generally symmetrical. In reality, bridge scour may have various different shapes. Among which, many scour holes are unsymmetrical. Therefore, these bridge scour models may fail to reflect the real scour situations perfectly. Rare attention has been paid to the effect of the unsymmetrical scour holes on the PNF in the previous studies. To address the need, scour scenarios with unsymmetrical scour holes were investigated in this study to investigate the change in the PNF, which is the first time that such an issue is discussed in the framework of PNF-based scour detection.

Fig. 9 illustrates an unsymmetrical scour hole development in the simulation. The soil around the pier in the upstream was removed with the same increment in each step; while the soil in the downstream remained unchanged in the first step, but was removed with the same increment as that in the upstream in the second step. In other words, the difference

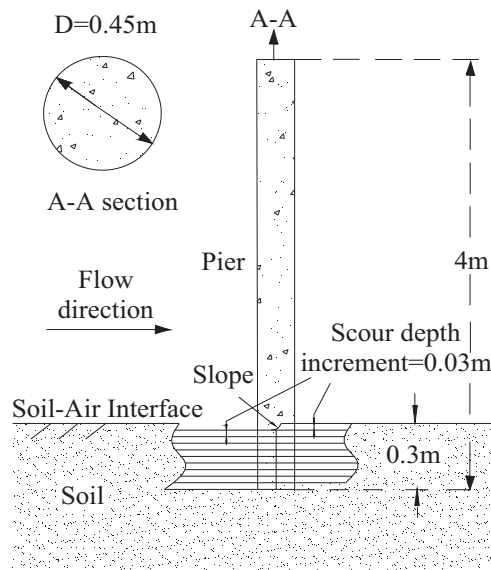


Fig. 9. Schematic of the unsymmetrical scour holes in the flow direction.

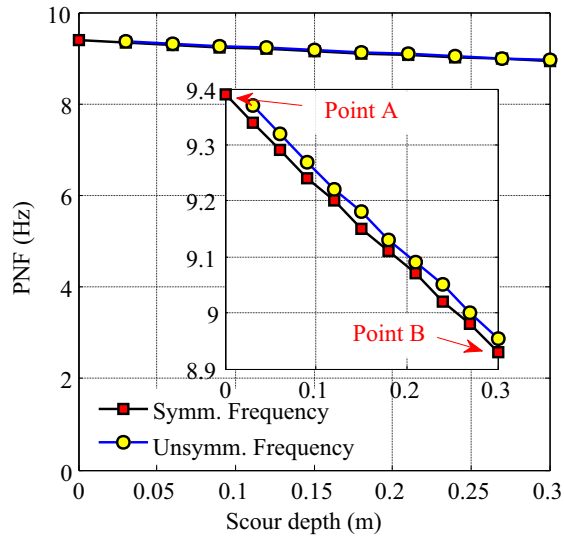


Fig. 10. Variation of the PNF with the symmetrical and unsymmetrical scour holes.

between the scour depths of the upstream and downstream soils remained 0.03 m to form the unsymmetrical scour holes at each scour level during the process. The interface between the upstream and the downstream was made to form a smooth slope (See Fig. 9) based on the experiment, which will be introduced in Section 4.3. The scour depth in the upstream was assumed as the scour depth for each unsymmetrical scour level. This section focused on scour progression developed from Point A to Point B in Fig. 4 where the experimental PNF decreased from 9.49 Hz to 8.97 Hz. Fig. 10 plots the variation of the PNF under the condition of the symmetrical and unsymmetrical scour holes. As can be seen, the PNF decreases with progressive scour for both the symmetrical and unsymmetrical scour holes. Therefore, bridge scour detection using the PNF still works in the unsymmetrical shape of scour holes, but attention is needed as the PNFs in the symmetrical and unsymmetrical scour holes are different. The reason is that the soils in the downstream of the pier provide more constraints in the downstream at each scour level with the unsymmetrical scour holes when compared to that with the symmetrical scour holes.

However, as the PNF variation is used to detect the scour depth, one question has to be posted, “What is the actual scour depth if one obtains the measured PNF in the field?” To be more specific, it is difficult to recognize that the measured PNF with an unsymmetrical scour hole corresponds to which specific scour depth, because the scour depths of the upstream and the downstream are not equal for an unsymmetrical scour hole. This question is significant because the scour depth is the most critical value in bridge maintenance. To solve this problem, a new criterion was proposed to define the scour depth

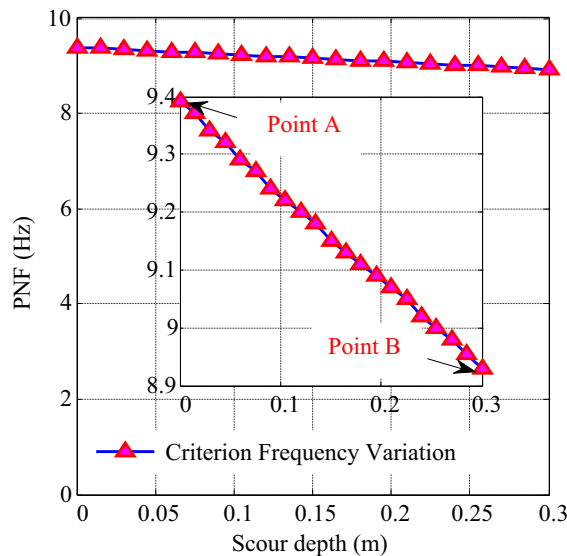


Fig. 11. Variation of the PNF with the symmetrical and unsymmetrical scour holes using the proposed criterion.

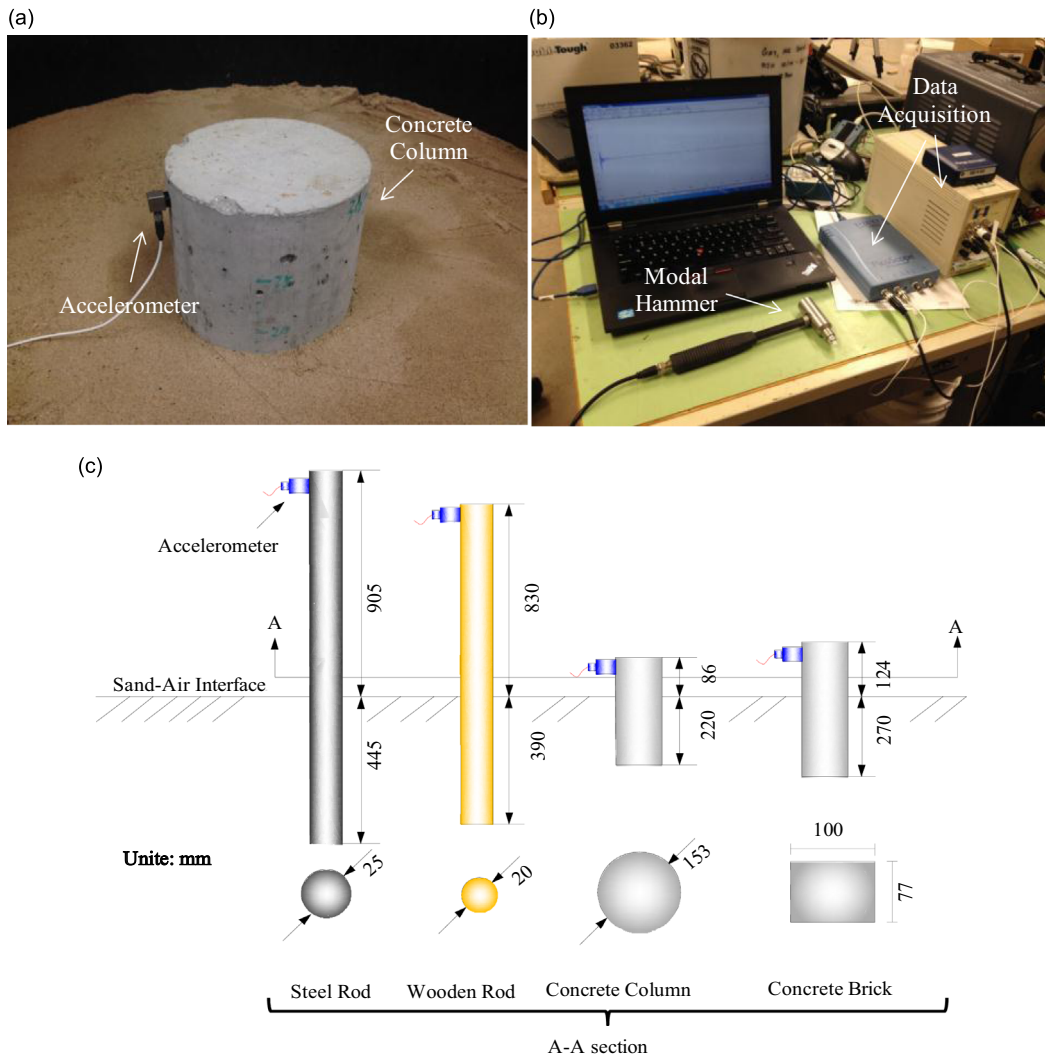


Fig. 12. Laboratory scour test: (a) test pier (b) data collection (c) schematic of the geometry of test piers.

Table 2

Geometries of the test piers and initial scour situations.

Test pier	Depth (mm)	Width/Length (mm)	Diameter (mm)	Embedded length (mm)	Scour increment (mm)	Sand relative density
Concrete column	306	–	153	220	30	Low
Concrete brick	394	77/100	–	270	30	Low
Steel rod	1350	–	25	445	30	High
Wooden rod	1220	–	20	390	50	High

with the unsymmetrical scour holes. For each unsymmetrical scour level, the average of the maximum (downstream) and the minimum (upstream) scour depth was assumed to be the actual scour depth for that unsymmetrical scour level. In other words, the actual scour depth of each unsymmetrical scour level is half of the original scour depth in Fig. 10. By using this criterion and combining the PNF obtained with the symmetrical scour holes, the variation of the PNF tends to be a smooth line as shown in Fig. 11. The result provided a way to address the critical problem caused by the unsymmetrical scour holes, that is, the variation of measured PNF from field tests is not smooth. This lays down the criterion for the implementations of PNF-based scour detection.

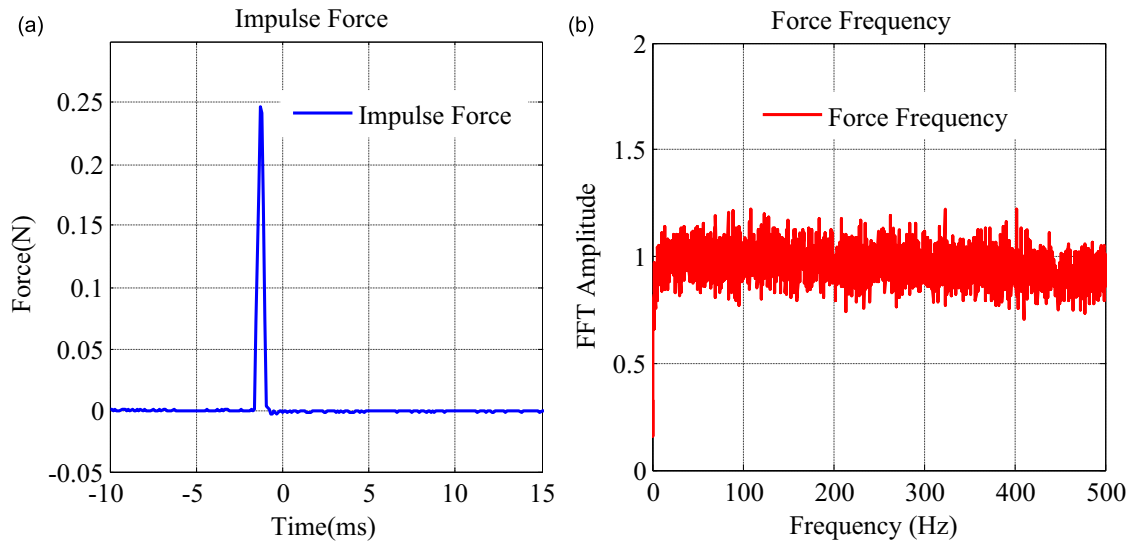


Fig. 13. Impulse force applied to the pier and its frequency.

## 4. Discussions based on experiments

### 4.1. A laboratory model

A laboratory-scale model of a single pier was constructed to validate the conclusions reached in the above discussions. A pier was installed in a sand matrix housed in a plastic tank. The tank is 520 mm, 855 mm, and 1280 mm in width, depth, and length, respectively. The tank was filled with play sands, which is uniformly graded. According to the previous studies [12,18,26], an accelerometer in this study was mounted at the location about 20 mm away from the top surface of the pier to record dynamic data as shown in Fig. 12a. The accelerometer was connected to the data acquisition as shown in Fig. 12b. A modal hammer was connected to the data acquisition to record signals of each impact. Dynamic signals of the pier and the modal hammer were recorded and then displayed on the computer screen using a digital oscilloscope. This software was implemented to take data samples at a scanning frequency of 10000 Hz, which provided adequate data for post-processing. The schematic of the geometry of each test pier is shown in Fig. 12c.

The vibration was generated by a transient force using the modal hammer. The force was applied on the plane where the accelerometer was fixed. The system responded instantly after the transient force was applied. The process of scour was produced by removing the sand around the pier. The initial scour level (Level 1) was the situation that there was no scour hole around the pier. The sand was removed in increments of 30 mm for the concrete column, concrete brick and steel rod, and 50 mm for the wooden rod to simulate different scour depths. The scour Level 6 was the final scour depth for each test pier for which 5 layers of soil had been removed. At each depth, the force was applied to generate free vibration and the accelerometer recorded the corresponding dynamic signals of the pier. The effect of water was not considered in this study, but sands around a bridge pier in most cases are under water in reality. To be realistic, the sand used in the test was maintained wet (the gravimetric water content is 5 percent).

Different shapes and material properties of the pier may have an effect on PNF-based scour detection. To reveal this effect, four types of piers were tested. The geometric properties and scour conditions of each are detailed in Table 2. For the wooden and steel rods, the sand was compacted in increments of 150 mm to obtain the 100 percent relative density of the sand. The purpose was to diminish the effect of loose sands on the rods caused by an impact. The sand used for the concrete column and brick was relatively loose. The loose sand was used to simulate the condition that the sand may be loose due to the saturated condition under water.

It is also necessary to minimize the contact duration between the hammer and the pier [16,27]. Fig. 13a and b depict a typical impulse force applied to the pier and its frequency spectrum, respectively. The contact duration is less than 2 ms and almost the same FFT amplitude was maintained within the duration, which implies that an ideal impulse was obtained as proposed in [16].

Fig. 14a and b show the dynamic responses of two types of piers at scour Level 1 and Level 6 in terms of acceleration. The acceleration contains a significant amount of high frequency vibration including assembled and superposed waveforms due to local effects [12,28]. The aim of this study is to extract the PNF of the pier to identify the scour depth, which is not relevant to the high frequency. For visualization, a low pass filter was applied to the signals of acceleration in Fig. 14a and b. A similar method was used in the study of Prendergast et al. [12]. The filtered signals are shown in Fig. 14c and d. The period between successive oscillations of scour Level 1 is larger than that of scour Level 6. The FFT was then used to obtain the PNF at each scour level for four types of piers. As shown in Fig. 15a, the PNF of the steel rod decreases from 8.4 Hz (Level 1) to 5.4 Hz

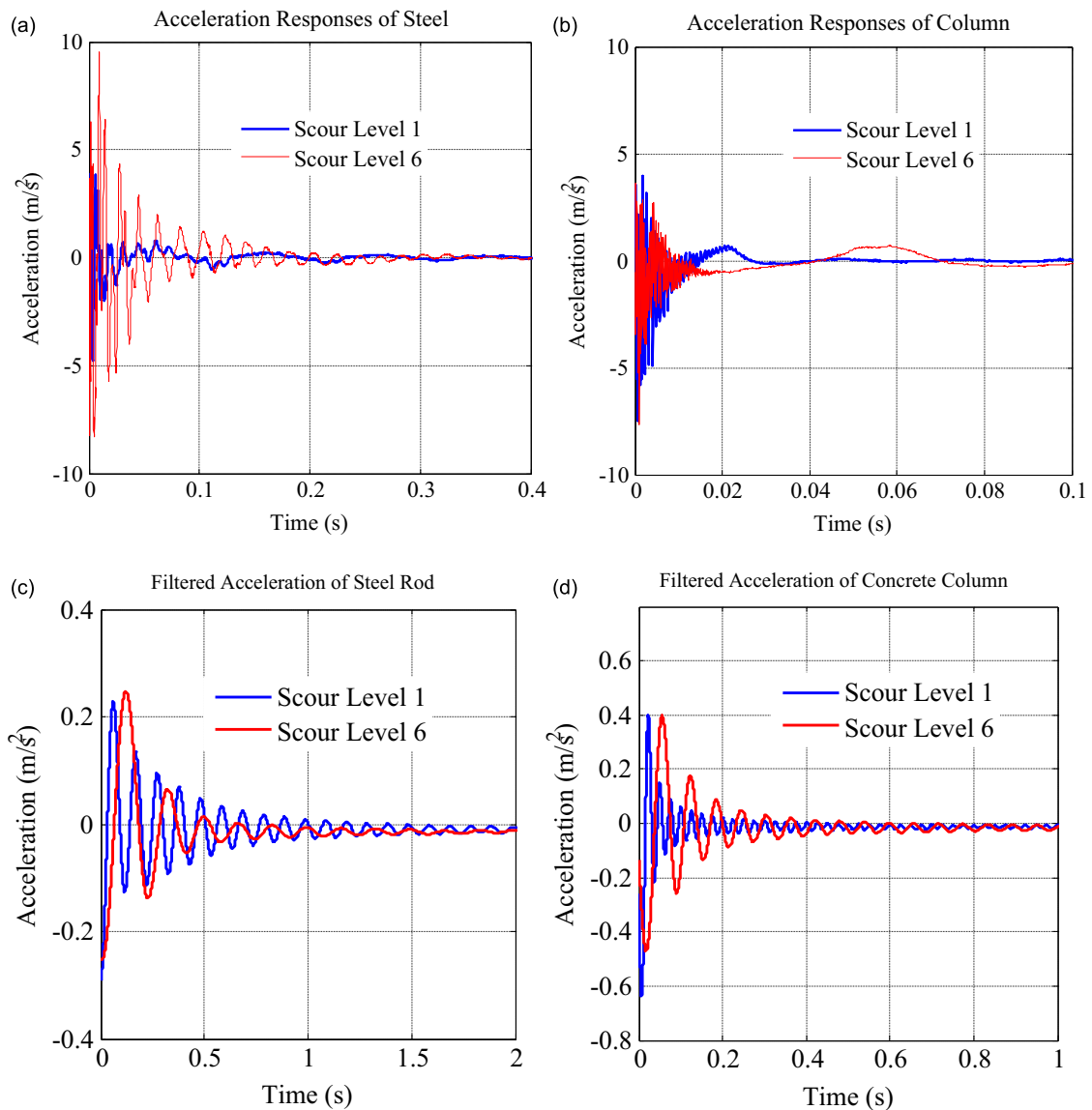


Fig. 14. Acceleration of the pier at scour Level 1 and Level 6.

(Level 6). A similar result was obtained in Fig. 15b for the concrete column, in which the PNF decreases from 37.3 Hz (Level 1) to 15.7 Hz (Level 6). During the entire test, there is a clear reduction in the PNF of the all types of piers (Fig. 15c).

#### 4.2. Validation of the location of sensor installation

The Laboratory test introduced in Section 4.1 was used to validate the conclusions made in Section 3.2 for the issue regarding the location of sensor installation. Two types of piers, i.e., the steel rod and the concrete column, were utilized to examine the difference of the PNFs measured with the accelerometer at different surface points of the piers. To this end, the accelerometer will be moving and deploying at the surfaces of the pier body in the horizontal and vertical directions. The PNF at each point will be obtained by analyzing its dynamic responses measured by the accelerometer using the FFT, but it is necessary to consider two factors, i.e., the contact between the sensor and the pier, and the impulse force. This is because the experiment will be tested by installing the accelerometer on one position then taking the accelerometer off to install it on another position with an impulse force generated by the modal hammer, which may cause experimental errors. Due to this concern, the sensitivity of these two factors was pre-investigated.

The effect of the impulse force was first examined using the steel rod. Once the accelerometer was mounted at Location 1, which was 40 mm away from the top surface of the pier at scour Level A, six artificial impulse forces were applied to generate the dynamic responses separately. The same procedure was undertaken when the sensor was removed to Location

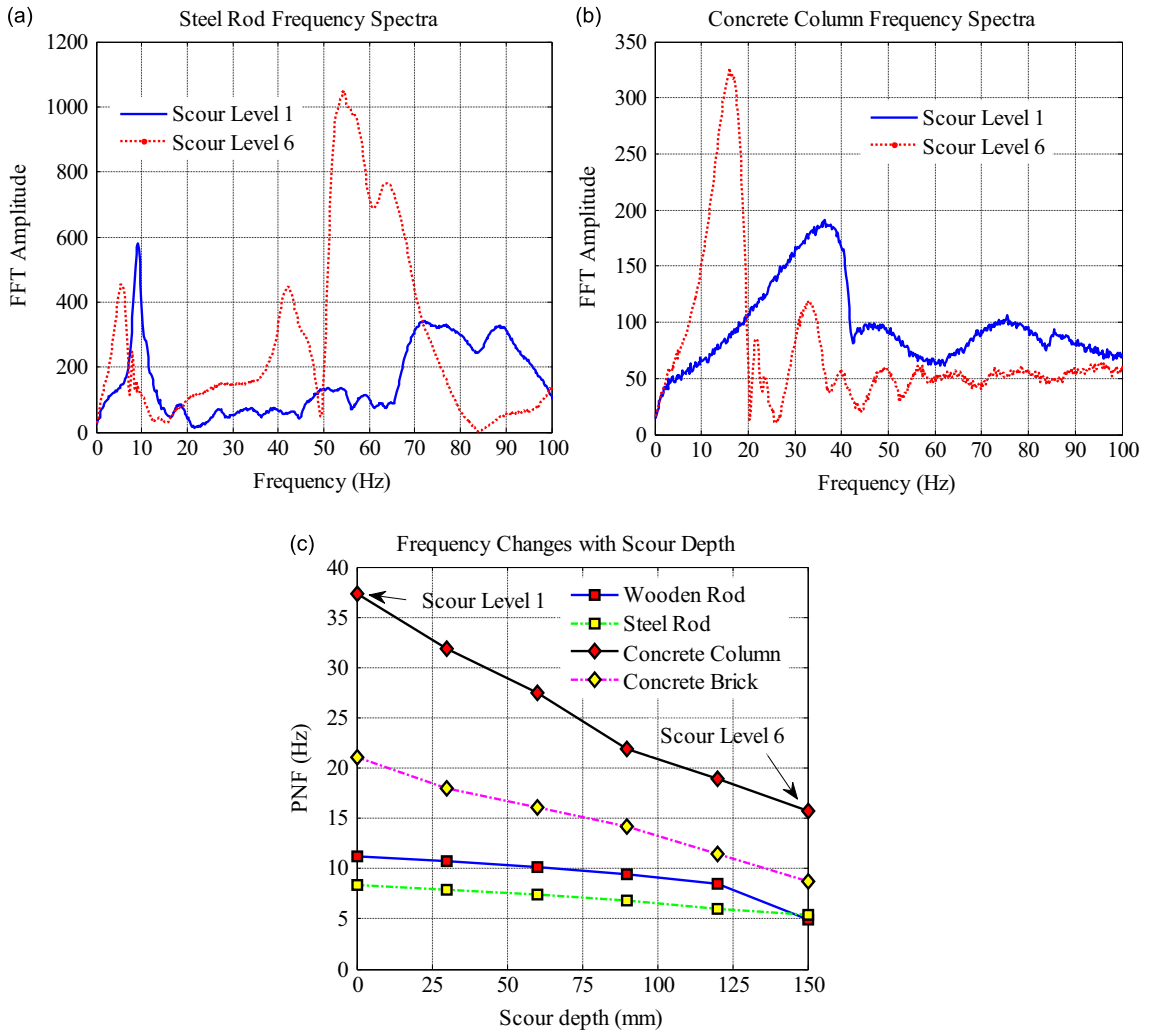


Fig. 15. Measured PNF: (a) PNF spectra of the steel rod; (b) PNF spectra of the concrete column; (c) variation of the PNFs of the four test piers.

**Table 3**  
Effect of the impulse force.

Scour	Random impulse force (N)	Location 1		Location 2		Location 3	
		Measured Freq. (Hz)	Avg. Freq.(Hz) ± Standard Dev.	Measured Freq. (Hz)	Avg. Freq.(Hz) ± Standard Dev.	Measured Freq.(Hz)	Avg. Freq.(Hz) ± Standard Dev.
Level A	0.0105	9.39	9.24 ± 0.11	9.39	9.28 ± 0.12	9.39	9.35 ± 0.08
	0.0116	9.39		9.39		9.39	
	0.0236	9.17		9.17		9.39	
	0.0216	9.17		9.39		9.39	
	0.0212	9.17		9.17		9.39	
	0.0190	9.17		9.17		9.17	
Level B	0.0249	8.8	8.67 ± 0.10	8.8	8.70 ± 0.11	8.8	8.77 ± 0.08
	0.0161	8.6		8.8		8.6	
	0.0254	8.8		8.8		8.8	
	0.0209	8.6		8.6		8.8	
	0.0128	8.6		8.6		8.8	
	0.0212	8.6		8.6		8.8	

2 and Location 3, which were 20 mm and 40 mm away from Location 1, respectively. To avoid the accidental deviation, the same procedure was implemented at scour Level B. The PNFs under different impulse forces were then compared. As shown in Table 3, the measured PNFs at Location 1 at scour Level A are very close, in which the maximum difference is 0.22 Hz and

**Table 4**  
Effect of the contact between the sensor and the pier.

Scour	Off-On counts	Location 1		Location 2		Location 3	
		Measured Freq.(Hz)	Avg. Freq.(Hz) ± Standard Dev.	Measured Freq. (Hz)	Avg. Freq.(Hz) ± Standard Dev.	Measured Freq.(Hz)	Avg. Freq.(Hz) ± Standard Dev.
Level A	1	9.11	9.22 ± 0.12	9.33	9.30 ± 0.08	9.39	9.37 ± 0.03
	2	9.11		9.33		9.32	
	3	9.11		9.33		9.39	
	4	9.32		9.33		9.33	
	5	9.32		9.33		9.39	
	6	9.32		9.13		9.39	
Level B	1	8.6	8.67 ± 0.10	8.6	8.73 ± 0.10	8.6	8.77 ± 0.08
	2	8.6		8.8		8.8	
	3	8.8		8.6		8.8	
	4	8.6		8.8		8.8	
	5	8.8		8.8		8.8	
	6	8.6		8.8		8.8	

the standard deviation is 0.11. Similar results were obtained at Locations 2 and 3 at scour Level A or scour Level B. Therefore, the PNFs at the same location have a minimal difference and the standard deviation is also minimal when six random impulse forces were applied, which indicates that the effect of the impulse force is negligible. The effect of the contact between the sensor and the pier was examined with the same concept and procedure. The only difference is that the sensor was taken off and on for six times at each position. Table 4 shows the PNF affected by the sensor contact. The PNF almost remains unchanged. The standard deviation at each position is less than 0.15 Hz, which reveals the negligible effect of the contact between the sensor and the pier.

Due to the negligible effects discussed above, the issue in Section 3.2 then was investigated by deploying the sensor at different designated positions on the pier body. The selected positions are illustrated in Fig. 6. Fig. 16 presents the experimental PNF along the horizontal and vertical directions of the pier body. The PNFs measured in the same horizontal plane almost remain unchanged as shown in Fig. 16a and c, which perfectly matches with the numerical solutions in Fig. 7. For the vertical direction, there is a slight difference in the PNF variation. The PNF variation in the numerical results in Fig. 8 is not smooth due to a jump, but the PNFs measured by the experiment in Fig. 16b and d increase gradually, which may be due to the local effects generated during the test. However, it is worthwhile to mention that the PNF measured at the top is greater than that at the bottom, which is in agreement with the numerical solutions. The results indicated that the optimal location of sensor installation should be as close as possible to the top surface of a pier. The reason is that the PMS such as the transverse bending of a pier, which corresponds to the PNF, is easier to be identified at the top than other positions due to the high amplitude of vibration. However, a real bridge pier connects with a bridge deck; as a result, the impedance from the bridge deck adding a mass and stiffness to the top of the pier may have a significant effect on the conclusion made in this study regarding the optimal location of sensor installation. Therefore, further research and precise experiments on a real structure are required to draw a more solid conclusion for that condition.

#### 4.3. Validation of the shape of scour holes

The conclusions regarding the influence of the shape of scour holes on the PNF were also validated using a laboratory test. To assess the shape of a typical scour hole, a bridge scour test was first performed. As shown in Fig. 17a, a fixed PVC pipe was embedded into the sands in the flume to simulate a bridge pier. The velocity of water was changed and used to scour the sands around the pipe. An unsymmetrical scour hole was finally formed as shown in Fig. 17a. The surface of the sands in the upstream is lower than that in the downstream, but the connection between the upstream and downstream is very smooth. Based on this evidence, the same unsymmetrical scour hole in the laboratory test was made artificially by removing the sands in the upstream; while the sands in the downstream remained unchanged. The test piers include the concrete brick and the concrete column as shown in Fig. 17b and c. To reproduce the scour hole as obtained in Fig. 17a, a smooth slope was made for the connection between the upstream and downstream. The procedure for producing an unsymmetrical scour hole was the same as that introduced in Section 3.3. The initial difference between scour depths in the upstream and downstream was 30 mm (upstream/downstream=0/30). This difference remained the same at each unsymmetrical scour level.

Fig. 18a plots the change in the PNF with the symmetrical and unsymmetrical scour holes. An explicit reduction in the PNF is observed due to scour development. Neglecting experimental deviations, the PNF variation with the symmetrical scour holes is parallel to that with unsymmetrical scour holes, which is in agreement with the numerical results in Fig. 10. Fig. 18b shows the adjusted PNFs using the criterion proposed in Section 3.3. The new PNF variation tends to be a smooth line, which confirmed the trend obtained in Fig. 11. This criterion is of practical significance as scour detection using the PNF of a pier would, in reality, takes place in conditions with both the symmetrical and unsymmetrical scour holes. Thus, the

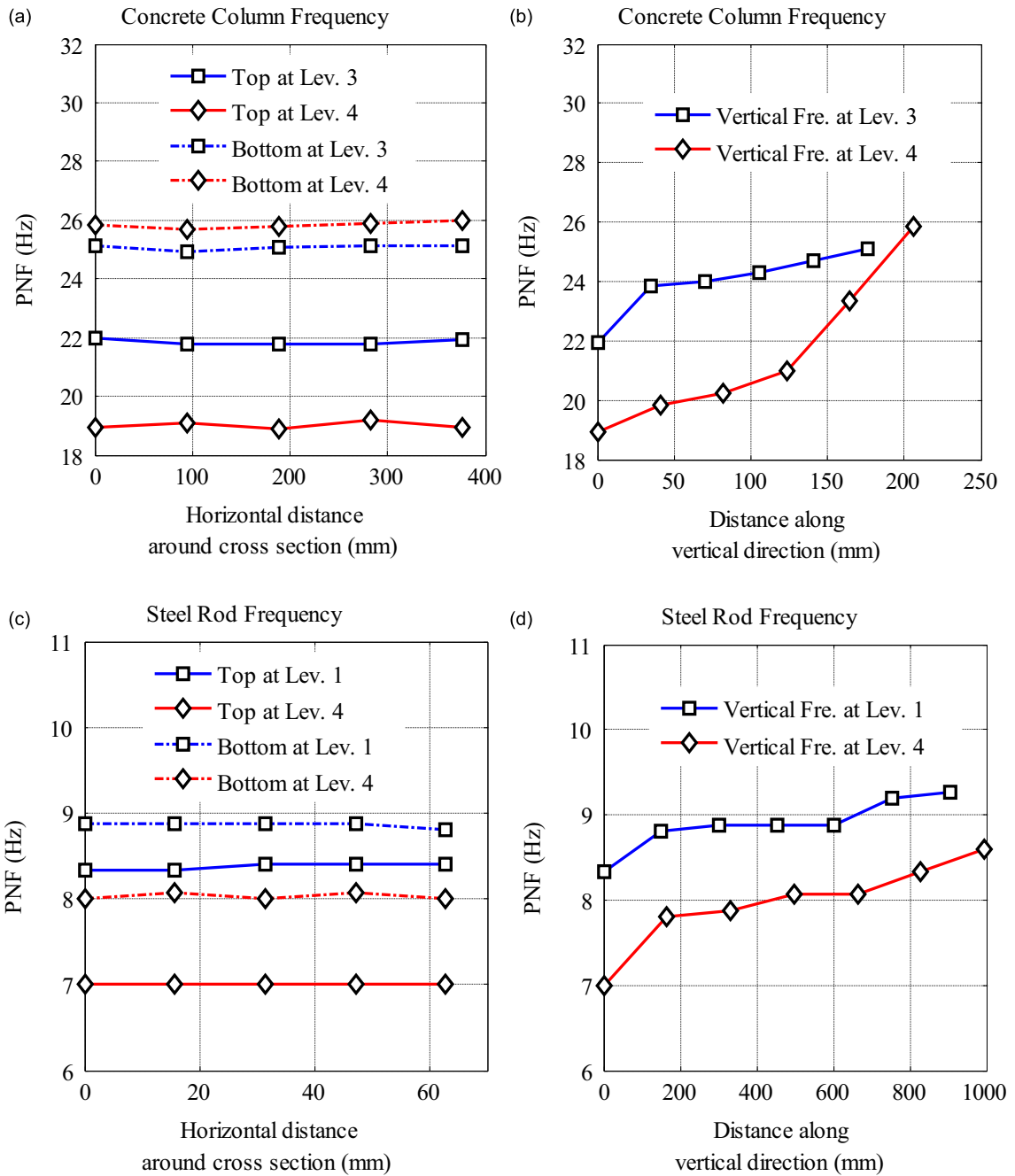


Fig. 16. Variation of the experimental PNF along the horizontal and vertical directions.

new criterion can be practically used to address problematic conditions in the field caused by the unsymmetrical scour holes, which advances the natural frequency spectrum-based scour detection framework.

### 5. Conclusions

A numerical model was developed to investigate the change in the PNF of a pier affected by progressive scour based on an existing laboratory scour test. Three unsolved but critical issues were discussed with simulations using this numerical model. Laboratory tests were then performed to validate the conclusions reached in the discussions based on the simulations, which shed light on both the theoretical basis and further implementations of PNF-based bridge scour detection.

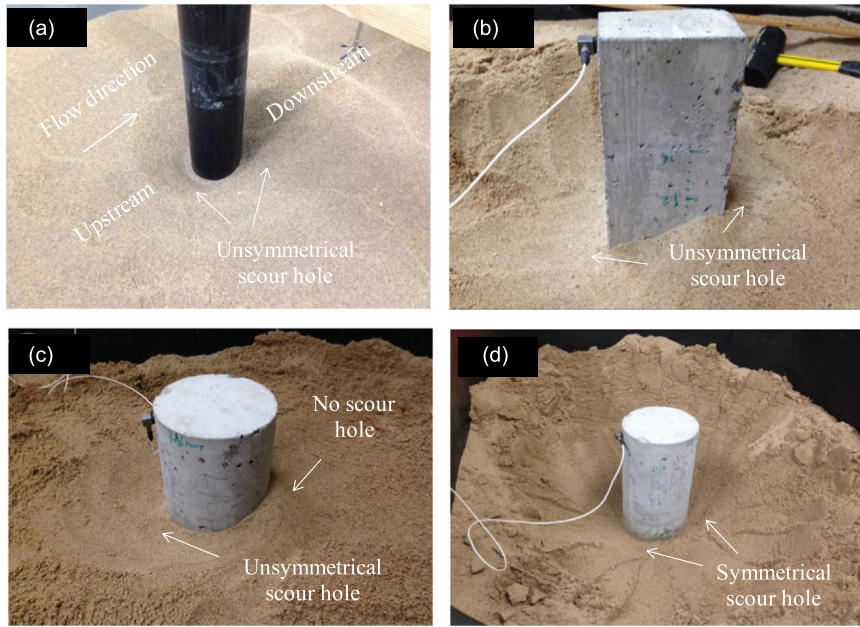


Fig. 17. Shape of scour holes test in progress.

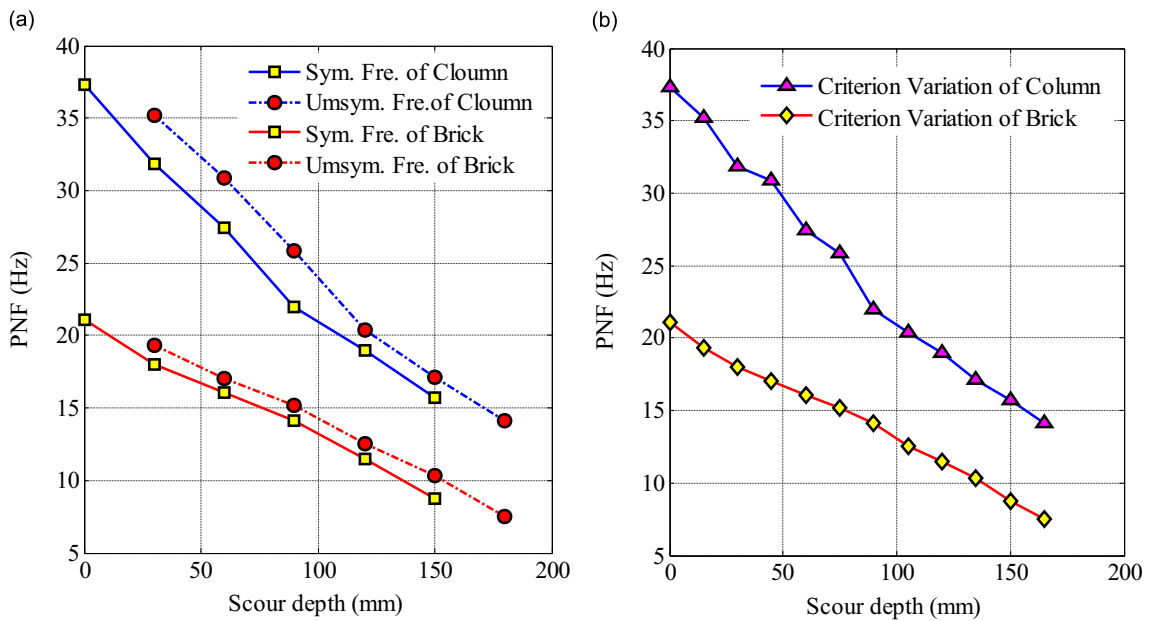


Fig. 18. Variation of the experimental PNF: (a) PNF variation with the symmetrical and unsymmetrical scour holes, (b) PNF variation using the criterion.

Based on the investigations, the following conclusions were obtained:

1. The way to know the physical meaning of the PNF identified from an eigenproblem with the soil-structure interaction has been verified by comparing the modal PNF with the dynamic PNF. This way can identify which PMS belongs to a bridge pier rather than the soils or the whole computational domain with minimal deviations.
2. The location of sensor installation has been evaluated by comparing the dynamic PNF measured at different points on the surface of the pier body in both the horizontal and vertical directions. The results confirmed that the measured PNFs remain unchanged in the same horizontal plane. However, the measured PNFs vary along the vertical (axial) direction. The value at the location close to the bottom of the pier is greater than that of the top. This indicated that the optimal location of sensor installation should be as close as possible to the top surface of a pier. The reason is that the PMS such as the transverse bending of a pier, which corresponds to the PNF, is more obvious at the top due to the high amplitude of

vibration. However, due to the fact that the effect of the bridge deck was not considered in the experiments, further research for a real structure is required to draw a more solid conclusion regarding the optimal location for sensor installation.

3. The influence of the shape of scour holes on the measured PNF of the pier has been investigated by developing scour scenarios with both the unsymmetrical and symmetrical scour holes. The results indicated that the PNF decreases with progressive scour for both the symmetrical and unsymmetrical scour holes, but the PNFs in the symmetrical and unsymmetrical scour holes are different due to different soil constraints.
4. A new criterion was proposed to define the scour depth with the unsymmetrical scour holes. By employing this criterion, the PNF variation tends to be a smooth line. Thus, this new criterion can be practically used to consider the unsymmetrical scour holes.

## Appendix A. Supplementary material

Supplementary data associated with this article can be found in the online version at <http://dx.doi.org/10.1016/j.jsv.2016.06.039>.

## References

- [1] K. Wardhana, F.C. Hadipriono, Analysis of recent bridge failures in the united states, *Journal of Performance of Constructed Facilities* 17 (2003) 144–150.
- [2] S.-Y. Lim, Equilibrium clear-water scour around an abutment, *Journal of Hydraulic Engineering* 123 (1997) 237–243.
- [3] B. Melville, A. Sutherland, Design method for local scour at bridge piers, *Journal of Hydraulic Engineering* 114 (1988) 1210–1226.
- [4] M. Najafzadeh, H.M. Azamathulla, Neuro-fuzzy gmdh to predict the scour pile groups due to waves, *Journal of Computing in Civil Engineering* (2013) 1–8.
- [5] S.-U. Choi, S. Cheong, Prediction of local scour around bridge piers using artificial neural networks, *Journal of the American Water Resources Association* 42 (2006) 487–494.
- [6] H. Zhu, X. Qi, P. Lin, Y. Yang, Numerical simulation of flow around a submarine pipe with a spoiler and current-induced scour beneath the pipe, *Applied Ocean Research* 41 (2013) 87–100.
- [7] M. Dixen, B.M. Sumer, J. Fredsøe, Numerical and experimental investigation of flow and scour around a half-buried sphere, *Coastal Engineering* 73 (2013) 84–105.
- [8] Z.G. Bai, R.C. Lv, R. Meng, Experimental investigation on scour around marine pipelines in silt beds by jet trenching, *Applied Mechanics and Materials* 256 (2013) 1956–1959.
- [9] Y.M. Hong, M.L. Chang, H.C. Lin, Y.C. Kan, C.C. Lin, Experimental study on clear water scour around bridge piers, *Applied Mechanics and Materials* 121 (2012) 162–166.
- [10] A. Zarafshan, A. Iranmanesh, F. Ansari, Vibration-based method and sensor for monitoring of bridge scour, *Journal of Bridge Engineering* 17 (2011) 829–838.
- [11] L. Prendergast, K. Gavin, A review of bridge scour monitoring techniques, *Journal of Rock Mechanics and Geotechnical Engineering* 6 (2014) 138–149.
- [12] L. Prendergast, D. Hester, K. Gavin, J. O'Sullivan, An investigation of the changes in the natural frequency of a pile affected by scour, *Journal of Sound and Vibration* 332 (2013) 6685–6702.
- [13] B. Hunt, *Monitoring scour critical bridges: a synthesis of highway practice*, Transportation Research Board of the National Academies, Washington, D.C., 2009, 1–158.
- [14] J.-L. Briaud, S. Hurlbaeus, K.-A. Chang, C. Yao, H. Sharma, O.-Y. Yu, C. Darby, B.E. Hunt, G.R. Price, Realtime monitoring of bridge scour using remote monitoring technology, No. FHWA/TX-11/0-6060-1, Texas Transportation Institute, Texas A&M University System, 2011, pp. 1–440.
- [15] N.L. Anderson, A.M. Ismael, T. Thitimakorn, Ground-penetrating radar: a tool for monitoring bridge scour, *Environmental Engineering Geoscience* 13 (2007) 1–10.
- [16] M. Shinoda, H. Haya, S. Murata, Nondestructive evaluation of railway bridge substructures by percussion test, *Proceedings of the Fourth International Conference on Scour and Erosion*, The Japanese Geotechnical Society, Tokyo, Japan, 2008, pp. 285–290.
- [17] S. Ju, Determination of scoured bridge natural frequencies with soil-structure interaction, *Soil Dynamics and Earthquake Engineering* 55 (2013) 247–254.
- [18] J.L. Briaud, C. Yao, C. Darby, H. Sharma, S. Hurlbaeus, G. Price, K. Chang, B. Hunt, O.Y. Yu, Motion sensors for scour monitoring: Laboratory experiments and numerical simulations, Transportation Research Board (TRB) 89th Annual Meeting, Transportation Research Board Washington, DC, 2010, pp. 1–22.
- [19] M. Samizo, S. Watanabe, T. Sugiyama, K. Okada, Evaluation of the structural integrity of bridge pier foundations using microtremors in flood conditions, *Proceedings of the International Conference on Scour and Erosion*, Scour and Erosion, San Francisco, CA, USA, 2010, pp. 824–833.
- [20] C. Yao, C. Darby, O.-Y. Yu, S. Hurlbaeus, K.-A. Chang, J. Price, B. Hunt, J.-L. Briaud, Motion sensors for scour monitoring: Laboratory experiment with a shallow foundation, GeoFlorida 2010: Advances in Analysis, Modeling & Design, GeoFlorida, West Palm Beach, USA, 2010, pp. 970–979.
- [21] R.R. Craig, A.J. Kurdila, *Fundamentals of Structural Dynamics*, John Wiley & Sons, New Jersey, 2006.
- [22] C. Lanczos, An iteration method for the solution of the eigenvalue problem of linear differential and integral operators, *Journal of Research of the National Bureau of Standards* 45 (1950) 255–282.
- [23] G. Gutenbrunner, K. Savov, H. Wenzel, Sensitivity studies on damping estimation, *Proceedings of the Second International Conference on Experimental Vibration Analysis for Civil Engineering Structures (EVACES)*, Porto, Portugal, 2007, pp. 1–9.
- [24] A.K. Chopra, *Dynamics of Structures*, Prentice Hall, New Jersey, 2006.
- [25] Y.W. Kwon, H. Bang, *The Finite Element Method Using Matlab*, CRC press, USA, 2000.
- [26] Y. Ko, W. Lee, W. Chang, H. Mei, C. Chen, Scour evaluation of bridge foundations using vibration measurement, *Proceedings of the fifth International Conference on Scour and Erosion*, San Francisco, CA, USA, 2010, pp. 884–893.
- [27] S. Foti, D. Sabia, Influence of foundation scour on the dynamic response of an existing bridge, *Journal of Bridge Engineering* 16 (2011) 295–304.
- [28] P.K. Roy, N. Ganesan, Transient response of a cantilever beam subjected to an impulse load, *Journal of Sound and Vibration* 183 (1995) 873–880.